Journal Pre-proofs

Lobaplatin induces pyroptosis through regulating cIAP1/2, Ripoptosome and ROS in nasopharyngeal carcinoma

Zide Chen, Gang Xu, Dong Wu, Shihai Wu, Long Gong, Zihuang Li, Guanghong Luo, Jian Hu, Jian Chen, Xiaoting Huang, Chengcong Chen, Zhenyou Jiang, Xianming Li

PII: S0006-2952(20)30250-1
DOI: https://doi.org/10.1016/j.bcp.2020.114023
Reference: BCP 114023

To appear in: *Biochemical Pharmacology*

Received Date: 6 March 2020
Accepted Date: 8 May 2020

Please cite this article as: Z. Chen, G. Xu, D. Wu, S. Wu, L. Gong, Z. Li, G. Luo, J. Hu, J. Chen, X. Huang, C. Chen, Z. Jiang, X. Li, Lobaplatin induces pyroptosis through regulating cIAP1/2, Ripoptosome and ROS in nasopharyngeal carcinoma, *Biochemical Pharmacology* (2020), doi: https://doi.org/10.1016/j.bcp.2020.114023

Lobaplatin induces pyroptosis through regulating cIAP1/2, Ripoptosome and ROS in nasopharyngeal carcinoma

Zide Chen[1,2], Gang Xu[1], Dong Wu[1], Shihai Wu[1], Long Gong[1], Zihuang Li[1,2], Guanghong Luo[1,2], Jian Hu[1,2], Jian Chen[2], Xiaoting Huang[3], Chengcong Chen[3], Zhenyou Jiang[2,*], Xianming Li[1,2,*]

[1]Department of Radiation Oncology, The 2nd Clinical Medical College (Shenzhen People's Hospital) of Jinan University, Shenzhen 518020, China

[2]Integrated Chinese and Western Medicine Postdoctoral Research Station, Jinan University, Guangzhou 510632, China

[3]Affiliated Cancer Hospital & Institute of Guangzhou Medical University, Guangzhou 510095, China.

Declaration of interest: none.

* **Correspondence:** Xianming Li, E-mail: lixianming1828@163.com or li.xianming@szhospital.com; Zhenyou Jiang, E-mail: tjzhy@jnu.edu.cn.

Abstract

Cisplatin is the most commonly used chemotherapeutic drug for nasopharyngeal carcinoma (NPC), while its side effects are often intolerable. Lobaplatin, as an effective third-generation platinum with fewer adverse reactions and less platinum cross-resistance, has been considered as a good alternative to cisplatin after cisplatin's failure (relapse or metastasis) in the treatment of NPC. However, the anti-NPC mechanism of lobaplatin remains largely unknown. In present study, 50% inhibiting concentration (IC50) of lobaplatin for NPC cells is found to be similar to that of cisplatin. 10 μM and 20 μM lobaplatin caused obvious gasdermin-E (GSDME)-mediated pyroptosis by activating caspase-3. Moreover, we found lobaplatin induced proteasomal degradation of cell inhibitor of apoptosis protein-1/2 (cIAP1/2). And these pyroptotic phenomena could be suppressed by the recovery of cIAP1/2, suggesting that cIAP1/2 are critical in lobaplatin-induced pyroptosis. Further inhibition of cIAP1/2 by birinapant (an antagonist of cIAP1/2) dramatically enhanced pyroptosis induced by lobaplatin *in vitro* and *in vivo*, which was consistent with the combination with cisplatin. Importantly, this synergistic pyroptotic effect were suppressed by the inhibition of Ripoptosome (RIPK1/Caspase-8/FADD), reactive oxygen species (ROS) and caspase-3 cleavage, and were independent of phosphorylation of JNK and NF-κB signal. Our data reveal that cIAP1/2 play important roles in lobaplatin-induced NPC cell pyroptosis, and this anti-NPC effect can be significantly potentiated by cIAP1/2 antagonist birinapant through regulating the formation of Ripoptosome and the generation of ROS. These study provides a possibility to further reduce the platinum-related adverse events and

chemoresistance of lobaplatin while maintaining satisfactory anti-NPC efficacy.

Keywords: Lobaplatin; Birinapant; cIAP1/2; Nasopharyngeal carcinoma; Pyroptosis

1. Introduction

Platinum-based combination therapy is recommended by the National Comprehensive Cancer Network (NCCN) as the first-line strategy for nasopharyngeal carcinoma (NPC) chemotherapy [1]. The most commonly used platinum in clinical practice is cisplatin. However, its toxicities, including nephrotoxicity, gastrointestinal upset, myelosuppression, ototoxicity, neurotoxicity and so on, are sometimes unbearable, which seriously affect patient compliance and standardization of the treatment, and might lead to chemoresistance and/or relapse of NPC [2-5]. Lobaplatin, as one of the third generation platinum, is recognized to have fewer adverse reactions, higher antitumor effect, less platinum cross-resistance, more soluble and stable in water [6, 7]. Nevertheless, the impact of potential dose-limiting thrombocytopenia of lobaplatin on patients still cannot be underestimated [6]. At present, lobaplatin is considered as an effective substitute platinum when cisplatin fails to treat NPC, such as relapse or metastasis [1]. However, its anti-NPC effect has not been compared with cisplatin yet, and its molecular mechanism remains obscure. Additionally, insensitivity of lobaplatin may still exist in some NPC cells. Thus, it is necessary to explore the mechanism of NPC resistance to lobaplatin and find a way to further reduce the dose-dependent

toxicity while ensuring its efficacy.

In current study, we demonstrated that lobaplatin induces pyroptosis, an inflammatory programme cell death, through regulating cell inhibitor of apoptosis protein-1/2 (cIAP1/2), Ripoptosome (RIPK1/Caspase-8/FADD) and reactive oxygen species (ROS) in NPC cells. And this anti-NPC effect of lobaplatin was significantly enhanced by birinapant, an antagonist of cIAP1/2 in clinical trials. These findings suggest that birinapant may be used to reduce the toxicity and improve the efficacy of lobaplatin.

2. Materials and Methods

2.1. Cell lines and reagents

NPC cell lines CNE-1 (catalog #JNO-1856), S26 (catalog #JNO-185), HONE-1 (catalog #JNO-1861), SUNE-1 (catalog #JNO-1860) and CNE-2 (catalog #JNO-1852), and non-tumor immortalized hepatocyte cell line HL-7702 (catalog #JNO-1738) were purchased from Guangzhou Tianjun Biological Technology Co., Ltd. (Guangzhou, GD, China). The cells were cultured in RPMI-1640 (Gibco, Waltham, MA, United States) supplemented with 10% fetal bovine serum (Gibco, Waltham, MA, United States) at 5% CO_2 and 37 ℃, and were routinely tested to ensure no mycoplasma contamination during the study. Birinapant, lobaplatin, cisplatin, ROS inhibitor NAC, c-Jun N-terminal kinase (JNK) inhibitor SP600125, nuclear factor kappa-B (NF-κB) inhibitor BMS-345541, RIPK3 inhibitor GSK'872, proteasome inhibitor MG-132 and chloroquine were purchased from SelleckChem (Houston, TX, United States). Pan-caspases inhibitor zVADfmk, caspase-8 specific inhibitor zIETDfmk, caspase-3

specific inhibitor zDEVDfmk were purchased from APExBIO (Houston, TX, United States). Small interfering RNA (siRNA) for RIPK1 (5'-AUCAAUCUGAGACUGUGUGAAGCCC-3'), caspase-3 (5'-CCGAAAGGUGGCAACAGAAUU-3') and scramble control siRNA were generated by IGEBIO (Guangzhou, GD, China). Plasmid pENTER-cIAP1 (catalog # CH877067), pENTER-cIAP2 (catalog # CH806295) and vehicle pENTER (catalog # PD88001) were purchased from Vigene Biosciences (Jinan, SD, China). Transfection reagent lipofectamine3000 was purchased from ThermoFisher Scientific (Waltham, MA, United States).

2.2. Cellular toxicity assays

Cell counting kit-8 (CCK-8, Dojindo, Kumamoto, Japan) assay was performed as previously described [8]. Briefly, cells were inoculated at a density of 6000 cells/well in 96-well plate, treated with birinapant and/or lobaplatin at the indicated concentrations for 24 or 48 hours before being assayed for cell viability. The microscopy imaging, lactate dehydrogenase (LDH) and IL-1β release assays were performed according to previous report [9].

2.3. Annexin-V/propidiumiodide (PI) apoptosis detection by flow cytometry

The annexin-V/PI (GeneCopoeia, Rockville, MD, United States) apoptosis detection were performed as previously described [10]. Briefly, cells were collected separately after different indicated treatments, and then incubated with Annexin V and PI dyes for 15 minutes in the dark. After detection by Accuri C6 flow cytometer (BD, Franklin

Lakes, NJ, United States), ratio of the dead cells was caculated by gating Annexin-V+/PI− and Annexin-V+/PI+.

2.4. Western blot and co-immunoprecipitation (CoIP)

Western blot and CoIP analyses were performed as previously described [11, 12]. Primary antibodies, including anti-cIAP1 (catalog #7065), anti-XIAP (catalog #2045), anti-caspase-8 (catalog #9746 and #4790), anti-caspase-3 (catalog #9662), anti-γH2AX (catalog #9718), anti-β-actin (catalog #4970), anti-p-JNK (catalog #4668), anti-JNK (catalog #9258), anti-p-p38 (catalog #9215), anti-p38 (catalog #9212), anti-p-IKBα (catalog #2859), anti-IKBα (catalog #9242), anti-NIK (catalog #4994), p100-52 (catalog #4882) and anti-FADD (catalog #2782) were purchased from CST (Danvers, MA, USA). Anti-NLRP3 (catalog #ab214185), anti-cIAP2 (catalog # ab32059), anti-ASC (catalog #ab155970), anti-caspase-1 (catalog #ab1872), anti-IL-1β (catalog #ab9722), anti-GSDME (catalog #ab215191), anti-GSDMD (catalog #ab210070) and anti-RIPK1 (catalog #ab72139) antibodies were obtained from Abcam (Cambridge, MA, USA).

2.5. Measurement of intracellular ROS

After stimulation with birinapant and/or lobaplatin for 24 hours, cells were stained with 10 μM 2',7'-Dichlorodihydrofluorescein diacetate (DCFH-DA) (NJJCBIO, Nanjing, China) for 1 hours at 37 °C in the dark. The level of ROS was measured by flow cytometer (BD, Franklin Lakes, NJ, USA).

2.6. Tumor xenografts

Female BALB/c nude mice (Guangdong Medical Laboratory Animal Center, China) aged 4 weeks were housed in a condition free of specific pathogens and implanted with 5×10^6 CNE-1 or S26 cells subcutaneously into the right axillary cavity. Body weight and tumor volume (length × width^2/2) were measured every 3 days. When tumors grew to 100 – 150 mm^3 in size, the mice were randomly divided into four groups, and were administered with birinapant (10 mg/kg, i.p., in 4% DMSO) every 3 days and/or lobaplatin (5 mg/kg, i.p. in PBS) every 6 days for 3 weeks. After execution by cervical dislocation, tumors, liver and kidneys of the mice were obtained. Pyroptosis were detected by Western blot using tumor tissue. Drug toxicities were measured by hematoxylin and eosin (H&E) staining analysis with liver and kidney tissues. The animal experiments were approved by the Animal Care and Ethics Committee, and were performed in accordance with the National Institutes of Health Guide for the Care and Use of Laboratory Animals (NIH Publications No. 8023, revised 1978).

2.7. Statistical analysis

Statistical comparisons were performed using two-way ANOVA followed by Dunnett's multiple comparisons test or Student's t-test by GraphPad Prism 6.0. *P*-values < 0.05 were considered statistically significant.

3. Results

3.1. Lobaplatin induces pyroptosis in NPC cell lines

In this study, CCK-8 assay showed that the inhibitory effect of lobaplatin on cell viability of five NPC cell lines is concentration-dependent and time-dependent (Fig. 1a-

1e). The IC50 values of lobaplatin in NPC cell lines were lower than that in immortalized hepatocyte cell line HL-7702 (Fig. 1a-1f and Table 1). Flow cytometry demonstrated that lobaplatin causes significant death of NPC cells (Fig. 1g and 1h). In addition, the activation of caspase-3 and the phosphorylation of H2AX at Ser139 (γH2AX), a well known marker of DNA double-stranded breaks (DSBs), were detected after 24 hours' stimulation of 10 μM and 20 μM lobaplatin (Fig. 1i).

Interestingly, lobaplatin induced balloon-like morphology of NPC cells, suggesting the possibility of pyroptosis (Fig. 1i). Pyroptosis, also known as secondary necrosis, is a form of inflammatory programmed cell death discovered in recent years [13]. It is mediated by different members of gasdermin superfamily, such as GSDMA, GADMB, GSDMC, GSDMD and GSDME [13]. Among them, GSDMD and GSDME can be cleaved and activated by caspase-1/-4/-5/-11 and caspase-3, respectively [14]. The N-terminal cleavage of these gasdermins is able to perforate the cell membrane and release inflammatory molecules (such as IL-1β) and other contents (such as LDH) outside the cell to induce inflammation, while promoting osmotic swelling of the cell [13]. In present study, Western blot, LDH and ELISA assays showed that GSDME (but not GSDMD) was activated, while cell content LDH and inflammatory factor IL-1β in NPC cells were released extracellularly, under the stimulation of lobaplatin (Fig. 1i-1l).

3.2. Pyroptosis induced by lobaplatin is via the proteasomal degradation of cIAP1/2 in NPC cell lines

cIAP1, cIAP2 and XIAP have been considered as negative regulators of cell death [15].

Western blot analysis showed that lobaplatin down-regulated the protein expression of cIAP1 and cIAP2 (cIAP1/2) with little effect on XIAP (Fig. 1i). Interestingly, the protein expression of cIAP1 and cIAP2 could be restored by proteasome inhibitor MG-132 instead of chloroquine (Fig. 2a), indicating their reduction is caused by proteasome degradation. Additionally, overexpression of cIAP1 or/and cIAP2 blocked the formation of free N-terminus of GSDME, and significantly inhibited the release of LDH and IL-1β (Fig. 2b-2f), which suggested that cIAP1/2 play key roles in the pyroptosis of NPC cells induced by lobaplatin.

3.3. cIAP1/2 antagonist birinapant and lobaplatin have a significant synergistic inhibitory effect on NPC cells

As mentioned above, the protein expression of cIAP1/2 could be down-regulated by lobaplatin, but not be completely inhibited even at a concentration of 20 μM (Fig.1i). We speculated that further degradation of cIAP1/2 might enhance the induction of pyroptosis of NPC cells by lobaplatin. Interestingly, we found birinapant, a well-known antagonist of cIAP1/2 [16], has a synergistic effect with lobaplatin on NPC cell activity (Fig. 3a-3f). Similarly, this synergistic effect also existed between birinapant and cisplatin on inhibiting the cell viability of NPC cell lines (Fig. 3g-3j). However, this synergistic effect was weak in the non-tumor immortalized cell line HL-7702 (Fig.3k). When birinapant and lobaplatin were used in combination, the protein expression of cIAP1/2 were almost undetectable (Fig. 4a), and the killing effect was highly elevated compared to the single agents (Fig. 4b-4c). Additionally, it was worth noting that birinapant also enhanced lobaplatin-induced pyroptotic events, including the generation

of free N-terminus of GSDME, the formation of balloon-like morphology of cells, and the release of LDH and IL-1β (Fig. 4a and Fig. 4d-4f).

It is reported that the release of IL-1β during pyroptosis requires activation of NLPR3 inflammasome composed of NLPR3, ASC and caspase-1 [17]. However, our research showed that both lobaplatin or/and birinapant failed to influence the signaling of NLRP3 inflammasome and the maturation of pro-IL-1β (Fig. 4g), suggesting other mechanisms may contribute to the release of IL-1β. Although similar balloon-like cell morphology also appears in necroptosis, this seems unlikely in this study, because GSK'872, a necropoptosis inhibitor, could not significantly reverse the inhibitory effect of birinapant and lobaplatin on NPC cells (Fig. 4h and 4i), which again indicated the occurrence of pyroptosis.

3.4. Pyroptosis of NPC cells induced by birinapant and lopaplatin is caspase dependent

In present study, the inhibitors of of pan-capsases (zVADfmk), caspase-8 (zIETDfmk) or caspase-3 (zDEVDfmk) efficiently reversed the inhibitory effect of birinapant and lobaplatin on NPC cells (Fig. 5a-5g). What was more, the blockade of pan-capsases, caspase-8 or caspase-3 reduced the generation of free N-terminus of GSDME, the release of LDH and IL-1β, and the formation of balloon-like morphology of NPC cells (Fig. 5b and Fig. 5e-5g), indicating that the pyroptosis of NPC cells induced by birinapant and lobaplatin is caspase-dependent.

3.5. Pyroptosis of NPC cells induced by birinapant and lobaplatin depends on ROS

and Ripoptosome

Pyroptosis induced by lobaplatin is reported to be via the ROS/JNK signaling pathway [9]. In current study, we found that birinapant and lobaplatin alone or in combination up-regulated ROS and phosphorylated JNK (pJNK) levels in NPC cells to a certain extent (Fig. 6a and 6b). However, JNK inhibitor SP600125 failed to reverse the inhibition of cell viability, and ROS scavenger NAC blocked a percentage of pyroptosis caused by the combination of birinapant and lobaplatin (Fig. 6c, 6d and 6g-6i). Thus, the generation of ROS may play a role in the pyroptosis induced by birinapant and lobaplatin.

Generally, the degradation of cIAP1/2 affects cell survival and death by regulating classical and non-classical NF-κB signaling [15]. Our research showed that birinapant alone or in combination with lobaplatin enhance the degradation of IKBα, and increase the protein levels of NIK and p52 (Fig. 6b), suggesting that both classical and non-classical NF-κB signaling pathways are activated, but the exact mechanism is still unclear. Besides, BMS-345541, an inhibitor of NF-κB signaling, did not inhibit, but further enhanced the killing effect of birinapant and lobaplatin on NPC cells (Fig. 6e and 6f). Therefore, pyroptosis in this study seems to be independent of NF-κB signaling, and it is likely to be caused by other mechanisms.

Ripoptosome, which contains receptor-interacting protein kinase 1 (RIPK1), Fas-associating protein with a novel death domain (FADD) and caspase-8, is a well-known platform that can manipulate the formation of apoptosis and necroptosis [18], but its role in pyroptosis is still unclear. In present study, CoIP assay showed that both

lobaplatin and birinapant alone induced the formation of Ripoptosome, which was more pronounced when they were used together (Fig. 7a). As a component, the knockdown of RIPK1 directly led to the inhibition of Ripoptosome formation (Fig. 7b). And these inhibitions partially blocked the killing effect of birinapant and lobaplatin (Fig. 7c and 7d), the cleavage of caspase-8 and caspase-3, as well as the expression of γH2AX (Fig. 7e). Moreover, these inhibitions of Ripoptosome also reduced the phenomena of pyroptosis, including the generation of free N-terminus of GSDME, the release of LDH and IL-1β, and the formation of balloon-like morphology of NPC cells, to some extent (Fig. 7f-7h). These data suggested that the pyroptosis of NPC cells induced by birinapant and lobaplatin partially depends on the formation of Ripoptosome. In addition, the clearance of ROS has little effect on the formation of Ripoptosome mediated by birinapant and lobaplatin (Fig. 7b), indicating the genaration of ROS may be downstream of Ripoptosome.

3.6. Birinapant enhances the inhibitory effect of lobaplatin on NPC xenografts

Finally, the *in vivo* anti-NPC effect of birinapant and lobaplatin was examined on CNE-1 and S26 tumor xenograft models (Fig. 8a-8j). Both birinapant and lobaplatin monotherapy reduced the growth of NPC xenografts, and the antitumor effect was significantly augmented when they were used in combination (Fig. 8a, 8b and Fig. 8e-8h). Western blot analysis showed that birinapant enhanced lobaplatin-induced downregulation of cIAP1/2, the activation of caspase-3 and GSDME, and the formation of γH2AX (Fig. 8i). Additionally, no significant changes in body weight were observed when mice were sacrificed (Fig. 8c and 8d). And H&E staining experiments showed

256 that birinapant and lobaplatin had no significant effect on the morphology of liver and
257 kidney tissues (Fig. 8j). These results suggested that mice might tolerate the
258 combination of birinapant and lobaplatin.

259 **4. Discussion**

260 Currently, the first-line chemotherapeutic drugs for clinical treatment of NPC are
261 platinums, of which the most commonly used is cisplatin [1]. However, the toxicity and
262 chemoresistance of cisplatin limit its application [2]. By contrast, lobaplatin is less toxic
263 and remains effective for NPCs that relapse or metastasize after cisplatin treatment [6,
264 7]. In this study, the anti-NPC effect of lobaplatin was similar to that of cisplatin,
265 unconsistent with the clinical report of cervical cancer and metastatic breast cancer [19,
266 20]. And our results suggest that loboplatin may be more targeted to NPC cells than
267 non-tumor cells, such as HL-7702 and mouse liver and kidney.
268 Generally, GSDME is widely expressed in normal cells, but is silent in most cancer
269 cells [21]. It can be specifically activated by the cleaved caspase-3 [22], and switches
270 caspase-3-mediated apoptosis induced by chemotherapy agents to pyroptosis [14]. Thus,
271 pyroptosis is thought to be faster and more thorough than apoptosis, and is usually
272 performed by activated GSDMD and/or GSDME [14]. Both free N-termini from
273 GSDMD and GSDME are able to perforate cell membranes, causing imbalance in
274 osmotic pressure of the cell [14]. We found that lobaplatin induces pyroptosis through
275 caspase-3/GSDME signaling pathway in NPC cells, just like in colorectal cancer [9].
276 However, GSDME rather than GSDMD underwent the cleavage and released the N-
277 terminus when NPC cells were stimulated by lobaplatin. Additionally, although

necroptosis can also cause balloon-like changes in cell morphology [23], and platinum can induce necroptosis in some certain cell types [24], this type of cell death was unlikely to occur in this study, because the necroptosis inhibitor GSK'872 could not reverse these changes in cell morphology.

Accumulating evidence indicates that IAPs, such as cIAP1, cIAP2, and XIAP, are a class of anti-apoptotic proteins that are commonly overexpressed in various malignancies and associated with treatment resistance and poor prognosis [15]. They play important roles in regulating cell death and survival [15]. The inhibition of IAPs reduce the characteristics of cancer stem cells and enhance the killing effect of some agents such as TNF-related apoptosis-inducing ligand (TRAIL) on NPC cells [25, 26]. Herein, we discovered that lobaplatin also down-regulate cIAP1/2 expression through protein degradation and their recovery can inhibit NPC cells from undergoing lobaplatin-induced pyroptosis. However, 10 μM and 20 μM lobaplatin did not completely inhibit the protein expression of cIAP1/2, suggesting that further inhibition of cIAP1/2 by their antagonists may enhance the anti-NPC effect of lobaplatin. In fact, in terms of reducing the side effects and chemoresistance of platinum for NPC, the NCCN recommends combining platinum with other therapies [1]. Nevertheless, due to the lack of large-scale phase III randomized clinical trials, the ideal combination strategy for NPC, especially for cisplatin and lobaplatin, is still being explored. Birinapant is one of the cIAP1/2 antagonists that can trigger the rapid proteasomal degradation of cIAP1/2 [16]. It is also an effective anti-tumor agent with a maximum tolerated dose of 47 mg/m^2 in humans [27], but its impact on NPC is still unknown. The

results of this study showed that both cisplatin and lobaplatin have a synergistic killing effect on NPC cells when combined with birinapant even at very low concentrations (e.g., 0.03125 μM), indicating cIAP1/2 antagonists may be good partners of platinum for the treatment of NPC.

Unlike previous studies that IAP antagonists enhance the apoptosis or necroptosis induced by cisplatin [25, 28], we found that birinapant alone also induce pyroptosis of NPC cells, and enhance lobaplaitn-induced pyroptosis. The activation of GSDME induced by birinapant and/or lobaplatin was demonstrated to be caused by the cleavage of caspase-3, which was impaired by caspase-8 inhibitor. These results indicate the activation of GSDME is via caspase-8/caspase-3.

cIAP1 and cIAP2 are capable of polyubiquitinating RIPK1, which promotes the formation of complexes leading to the activation of classic NF-κB signaling pathway and ultimately regulates cell survival [15]. However, when cIAP1 and cIAP2 are eliminated, RIPK1 lacking polyubiquitination does not activate the classic NF-κB signal, but forms a Ripoptosome with caspase-8 and FADD to trigger cell death [15]. The formation of Ripoptosome was detected when NPC cells were stimulated with birinapant and/or lobaplatin. Knockdown of RIPK1 inhibited the formation of Ripoptosome and the activation of caspase-8, caspase-3 and GSDME, suggesting that the activation of GSDME induced by birinapant and/or lobaplatin is through Ripoptosome/caspase-3 signaling pathway.

Upregulation of ROS and pJNK are considered to be the main mechanisms of lobaplatin-induced pyroptosis in colon cancer [9]. However, the inhibition of pJNK did

not effectively block the inhibitory effect of birinapant and lobaplatin on NPC in our study. And the clearance of ROS only partially inhibited the NPC pyroptosis induced by birinapant and lobaplatin. These differences in molecular mechanisms may be due to the heterogeneity between different types of cancer [29]. We noticed that birinapant activated both classical and non-classical NF-κB signaling in NPC cells, which is consistent with previous reports [16]. However, the blockade of the NF-κB signal did not inhibit but accelerated pyroptosis induced by birinapant and lobaplatin. Therefore, targeting NF-κB may be a way to further improve the efficacy of lobaplatin against NPC and reduce platinum-related side effects.

In conclusion, lobaplatin increases the GSDME-mediated pyroptosis of NPC cells by inducing the degradation of cIAP1/2. And birinapant potentiates the cytotoxic effect of lobaplatin on NPC cells *in vitro* and *in vivo*, which is via regulating the formation of Ripotosome/ROS/caspase-3. Our data suggest that the application of cIAP1/2 antagonists and lobaplatin may lower the platinum related adverse events and chemoresistance during NPC treatment, however more evidence is required.

Acknowledgements

This work was supported by grants from the China Postdoctoral Science Foundation (grant numbers 2019M663396) and the Special Foundation for the Development of Strategic Emerging Industries of Shenzhen (grant numbers JCYJ20180228175652675).

Conflict of interests

All authors have no conflict of interest to this work.

Ethics approval

The manuscript did not contain clinical studies or patient data. All animal experiments were approved by the Animal Care and Ethics Committee, and followed the National Institutes of Health Guide for the Care and Use of Laboratory Animals (NIH Publications No. 8023, revised 1978).

References

[1] D. Adelstein, M.L. Gillison, D.G. Pfister, S. Spencer, D. Adkins, D.M. Brizel, B. Burtness, P.M. Busse, J.J. Caudell, A.J. Cmelak, A.D. Colevas, D.W. Eisele, M. Fenton, R.L. Foote, J. Gilbert, R.I. Haddad, W.L. Hicks, Y.J. Hitchcock, A. Jimeno, D. Leizman, W.M. Lydiatt, E. Maghami, L.K. Mell, B.B. Mittal, H.A. Pinto, J.A. Ridge, J. Rocco, C.P. Rodriguez, J.P. Shah, R.S. Weber, M. Witek, F. Worden, S.S. Yom, W. Zhen, J.L. Burns, S.D. Darlow, NCCN Guidelines Insights: Head and Neck Cancers, Version 2.2017, J Natl Compr Canc Netw 15(6) (2017) 761-770.

[2] K. Barabas, R. Milner, D. Lurie, C. Adin, Cisplatin: a review of toxicities and therapeutic applications, Vet Comp Oncol 6(1) (2008) 1-18.

[3] X. Wang, X. Wang, Z. Guo, Functionalization of Platinum Complexes for Biomedical Applications, Acc Chem Res 48(9) (2015) 2622-31.

[4] S.L. Liu, X.S. Sun, J.J. Yan, Q.Y. Chen, H.X. Lin, Y.F. Wen, S.S. Guo, L.T. Liu, H.J. Xie, Q.N. Tang, Y.J. Liang, X.Y. Li, C. Lin, Y.Y. Du, Z.C. Yang, B.B. Xiao, J.H. Yang, L.Q. Tang, L. Guo, H.Q. Mai, Optimal cumulative cisplatin dose in nasopharyngeal carcinoma patients based on induction chemotherapy response, Radiother Oncol 137 (2019) 83-94.

[5] C.J. Tao, L. Lin, G.Q. Zhou, L.L. Tang, L. Chen, Y.P. Mao, M.S. Zeng, T.B. Kang, W.H. Jia, J.Y. Shao, H.Q. Mai, A.H. Lin, J. Ma, Y. Sun, Comparison of long-term survival and toxicity of cisplatin delivered weekly versus every three weeks concurrently with intensity-modulated radiotherapy in nasopharyngeal carcinoma, PLoS One 9(10) (2014) e110765.

[6] L.R. Ke, W.X. Xia, W.Z. Qiu, X.J. Huang, J. Yang, Y.H. Yu, H. Liang, G.Y. Liu, Y.F. Ye, Y.Q. Xiang, X. Guo, X. Lv, Safety and efficacy of lobaplatin combined with 5-fluorouracil as first-line induction chemotherapy followed by lobaplatin-radiotherapy in locally advanced nasopharyngeal carcinoma: preliminary results of a prospective phase II trial, BMC Cancer 17(1) (2017) 134.

[7] G.X. Long, J.W. Lin, D.B. Liu, X.Y. Zhou, X.L. Yuan, G.Y. Hu, Q. Mei, G.Q. Hu, Single-arm, multi-centre phase II study of lobaplatin combined with docetaxel for recurrent and metastatic nasopharyngeal carcinoma patients, Oral Oncol 50(8) (2014) 717-20.

[8] J. Chen, W. Li, K. Cui, K. Ji, S. Xu, Y. Xu, Artemisitene suppresses tumorigenesis by inducing DNA damage through deregulating c-Myc-topoisomerase pathway, Oncogene 37(37) (2018) 5079-5087.

[9] J. Yu, S. Li, J. Qi, Z. Chen, Y. Wu, J. Guo, K. Wang, X. Sun, J. Zheng, Cleavage of GSDME by caspase-3 determines lobaplatin-induced pyroptosis in colon cancer cells, Cell Death Dis 10(3) (2019) 193.

[10] Z. Chen, J. Chen, H. Liu, W. Dong, X. Huang, D. Yang, J. Hou, X. Zhang, The SMAC Mimetic APG-1387 Sensitizes Immune-Mediated Cell Apoptosis in Hepatocellular Carcinoma, Front Pharmacol 9 (2018) 1298.

[11] Z. Chen, W. Zhuang, Z. Wang, W. Xiao, W. Don, X. Li, X. Chen, MicroRNA-450b-3p inhibits cell growth by targeting phosphoglycerate kinase 1 in hepatocellular carcinoma, J Cell Biochem 120(11) (2019) 18805-18815.

[12] N. Li, L. Feng, H.Q. Han, J. Yuan, X.K. Qi, Y.F. Lian, B.H. Kuang, Y.C. Zhang, C.C. Deng, H.J. Zhang, Y.Y. Yao, M. Xu, G.P. He, B.C. Zhao, L. Gao, Q.S. Feng, L.Z. Chen, L. Yang, D. Yang, Y.X. Zeng, A novel Smac mimetic APG-1387 demonstrates potent antitumor activity in nasopharyngeal carcinoma cells by inducing apoptosis, Cancer Lett 381(1) (2016) 14-22.

[13] S. Feng, D. Fox, S.M. Man, Mechanisms of Gasdermin Family Members in Inflammasome Signaling and Cell Death, J Mol Biol 430(18 Pt B) (2018) 3068-3080.

[14] S.B. Kovacs, E.A. Miao, Gasdermins: Effectors of Pyroptosis, Trends Cell Biol 27(9) (2017) 673-684.

[15] A. Derakhshan, Z. Chen, C. Van Waes, Therapeutic Small Molecules Target Inhibitor of Apoptosis Proteins in Cancers with Deregulation of Extrinsic and Intrinsic Cell Death Pathways, Clin Cancer Res 23(6) (2017) 1379-1387.

[16] E. Varfolomeev, J.W. Blankenship, S.M. Wayson, A.V. Fedorova, N. Kayagaki, P. Garg, K. Zobel, J.N. Dynek, L.O. Elliott, H.J. Wallweber, J.A. Flygare, W.J. Fairbrother, K. Deshayes, V.M. Dixit, D. Vucic, IAP antagonists induce autoubiquitination of c-IAPs, NF-kappaB activation, and TNFalpha-dependent apoptosis, Cell 131(4) (2007) 669-81.

[17] H. Hao, L. Cao, C. Jiang, Y. Che, S. Zhang, S. Takahashi, G. Wang, F.J. Gonzalez, Farnesoid X Receptor Regulation of the NLRP3 Inflammasome Underlies Cholestasis-Associated Sepsis, Cell Metab 25(4) (2017) 856-867 e5.

[18] M. Feoktistova, P. Geserick, D. Panayotova-Dimitrova, M. Leverkus, Pick your poison: the Ripoptosome, a cell death platform regulating apoptosis and necroptosis, Cell Cycle 11(3) (2012) 460-7.

[19] J.Q. Wang, T. Wang, F. Shi, Y.Y. Yang, J. Su, Y.L. Chai, Z. Liu, A Randomized Controlled Trial Comparing Clinical Outcomes and Toxicity of Lobaplatin- Versus Cisplatin-Based Concurrent Chemotherapy Plus Radiotherapy and High-Dose-Rate Brachytherapy for FIGO Stage II and III Cervical Cancer, Asian Pac J Cancer Prev 16(14) (2015) 5957-61.

[20] Z. Wang, L. Xu, H. Wang, Z. Li, L. Lu, X. Li, Q. Zhang, Lobaplatin-based regimens outperform cisplatin for metastatic breast cancer after anthracyclines and taxanes treatment, Saudi J Biol Sci 25(5) (2018) 909-916.

[21] Y. Wang, W. Gao, X. Shi, J. Ding, W. Liu, H. He, K. Wang, F. Shao, Chemotherapy drugs induce pyroptosis through caspase-3 cleavage of a gasdermin, Nature 547(7661) (2017) 99-103.

[22] C. Rogers, T. Fernandes-Alnemri, L. Mayes, D. Alnemri, G. Cingolani, E.S. Alnemri, Cleavage of DFNA5 by caspase-3 during apoptosis mediates progression to secondary necrotic/pyroptotic cell death, Nat Commun 8 (2017) 14128.

[23] Y. Zhang, X. Chen, C. Gueydan, J. Han, Plasma membrane changes during programmed cell deaths, Cell research 28(1) (2018).

[24] Y. Xu, H.-B. Ma, Y.-L. Fang, Z.-R. Zhang, J. Shao, M. Hong, C.-J. Huang, J. Liu, R.-Q. Chen, Cisplatin-induced necroptosis in TNFα dependent and independent pathways, Cellular signalling 31 (2017) 112-123.

[25] M.S. Wu, G.F. Wang, Z.Q. Zhao, Y. Liang, H.B. Wang, M.Y. Wu, P. Min, L.Z. Chen, Q.S. Feng, J.X. Bei, Y.X. Zeng, D. Yang, Smac mimetics in combination with TRAIL selectively target cancer stem cells in nasopharyngeal carcinoma, Mol Cancer Ther 12(9) (2013) 1728-37.

[26] J. Ji, Y. Yu, Z.L. Li, M.Y. Chen, R. Deng, X. Huang, G.F. Wang, M.X. Zhang, Q. Yang, S. Ravichandran, G.K. Feng, X.L. Xu, C.L. Yang, M.Z. Qiu, L. Jiao, D. Yang, X.F. Zhu, XIAP Limits Autophagic Degradation of Sox2 and Is A Therapeutic Target in Nasopharyngeal Carcinoma Stem Cells, Theranostics 8(6) (2018) 1494-1510.

[27] A.M. Noonan, K.P. Bunch, J.Q. Chen, M.A. Herrmann, J.M. Lee, E.C. Kohn, C.C. O'Sullivan, E. Jordan, N. Houston, N. Takebe, R.J. Kinders, L. Cao, C.J. Peer, W.D. Figg, C.M. Annunziata, Pharmacodynamic markers and clinical results from the phase 2 study of the SMAC mimetic birinapant in women with relapsed platinum-resistant or -refractory epithelial ovarian cancer, Cancer 122(4) (2016) 588-597.

[28] K.E. McCabe, K. Bacos, D. Lu, J.R. Delaney, J. Axelrod, M.D. Potter, M. Vamos, V. Wong, N.D. Cosford, R. Xiang, D.G. Stupack, Triggering necroptosis in cisplatin and IAP antagonist-resistant ovarian carcinoma, Cell Death Dis 5 (2014) e1496.

436 [29] H. D, W. RA, Hallmarks of cancer: the next generation, Cell 144(5) (2011) 646-74.

437

438

Figure legends

Fig. 1 Lobaplatin induces pyroptosis in NPC cell lines.

(a-f) NPC cell lines CNE-1, S26, HONE-1, SUNE-1 and CNE-2, and non-tumor immortalized hepatocyte cell line HL-7702 were treated with lobaplatin at indicated concentrations for 24 or 48 hours, followed by CCK8 assay for cell viability analysis. **(g, h)** CNE-1 and S26 cell lines were treated with indicated concentrations of lobaplatin for 24 hours, then the ratio of cell death was analyzed by flow cytometry. **(i)** Gel images of total and cleaved caspase-3 (cas-3 and cl-cas-3), full length and free N-ternimus of GSDME (GSDME-F and GSDME-N), full length and free N-ternimus of GSDMD (GSDMD-F and GSDMD-N), total and cleaved caspase-1 (cas-1 and cl-cas-1), γH2AX, cIAP1, cIAP2 and XIAP were obtained by Western blot. **(j)** Balloon-like cell morphology was shown by bright-field microscopy. **(k)** LDH and **(l)** IL-1β levels in the culture supernatant were detected by LDH kit and IL-1β ELISA kit, respectively. Experiments were repeated three times independently. Ctrl, control. L10, 10 μM lobaplatin; L20, 20 μM lobaplatin. * , $P < 0.05$ compared with the control group. #, $P < 0.05$ compared with the '24 hours' group.

Fig. 2 Lobaplatin induces proteasomal degradation of cIAP1/2 in NPC cell lines.

(a) CNE-1 and S26 cells were pretreated with proteasesome inhibitor chloroquine (CQ, 20 μM) and/or MG-132 (10 μM) for 30 minutes and then stimulated with 10 μM lobaplatin for 24 hours, the degradation of cIAP1/2 was measured by Western blot. **(b, c)** The over-expression plasmids pENTER-cIAP1 or/and pENTER-cIAP2 were

461 transfected into CNE1 or S26 cells, and then stimulated with 20 μM lobaplatin for 24
462 hours, **(d)** the full length and free N-ternimus of GSDME (GSDME-F and GSDME-N)
463 were detected by Western blot, **(e, f)** and the levels of LDH and IL-1β in the culture
464 supernatant were measured by LDH kit and IL-1β ELISA kit, respectively. Ctrl, control.
465 L10, 10 μM lobaplatin; L20, 20 μM lobaplatin. pENTER, vehicle. * , $P < 0.05$.
466

467 **Fig. 3 Birinapant and platinums have a significant synergistic inhibitory effect on**
468 **NPC cell viability.**

469 **(a-e)** NPC cell lines CNE-1, S26, HONE-1, SUNE-1 and CNE-2 were treated with
470 indicated concentrations of birinapant alone or in combination with lobaplatin for 24 or
471 48 hours and then analyzed for cell viability. **(f)** Combination index between lobaplatin
472 and birinapant was calculated using CompuSyn software. Combination index values of
473 less than 1.0 or more than 1.0 were synergistic or antagonistic, respectively. **(g-i)** NPC
474 cell lines CNE-1 and S26 were treated with indicated concentrations of birinapant alone
475 or in combination with cisplatin for 24 or 48 hours and then analyzed for cell viability,
476 and **(j)** the combination index between cisplatin and birinapant was calculated using
477 CompuSyn software. **(k)** Combination index between lobaplatin and birinapant in non-
478 tumor immortalized hepatocyte cell line HL-7702 was calculated using CompuSyn
479 software. Experiments were repeated three times independently. Ctrl, control.
480 L0/5/10/20/40, represented 0, 5, 20, 20, 40 μM lobaplatin. C0/5/10/20/40, represented
481 0, 5, 20, 20, 40 μM cisplatin. * , $P < 0.05$ compared with the 'L0 (24h)' or 'C0 (24h)'
482 group.

Fig. 4 Birinapant enhances NPC cell pyroptosis induced by lobaplatin *in vitro*.

CNE-1 and S26 cells were treated with 1 μM birinapant (B1), 10 μM lobaplatin (L10), or both (B1L10) for 24 hours. **(a, g)** Gel images of cIAP1, cIAP2, XIAP, total and cleaved caspase-8 (cas-8 and cl-cas-8), total and cleaved caspase-3 (cas-3 and cl-cas-3), γH2AX, full length and free N-ternimus of GSDME (GSDME-F and GSDME-N), NLRP3, ASC, total and cleaved caspase-1 (cas-1 and cl-cas-1), prototype and mature IL-1β, full length and free N-ternimal of GSDMD were obtained through Western blot analysis. (**b, c**) Dead ratios of CNE-1 and S26 cells were detected by annexin V/PI cytometry. **(d)** Balloon-like cell morphology was shown by bright-field microscopy. **(e)** LDH and **(f)** IL-1β levels were measured with culture supernatant. **(h, i)** CNE-1 and S26 cells were treated with 1 μM birinapant (B1) and 10 μM lobaplatin (L10) in the presence or absence of necroptosis inhibitor (GSK'872, 2 μM) for 24 hours. **(h)** Cell viability was measured via CCK-8 assay. **(i)** LDH level was measured with culture supernatant. Experiments were repeated three times independently. Ctrl, control. * , $P < 0.05$. PC, positive control.

Fig. 5 Pyroptosis of NPC cells induced by birinapant and lopaplatin is caspase-dependent.

CNE-1 and S26 cells were treated with 1 μM birinapant (B1) and 10 μM lobaplatin (L10) in the presence or absence of pan-caspases inhibitor (zVADfmk, 100 μM), caspase-8 specific inhibitor (zIETDfmk, 100 μM), caspase-3 specific inhibitor

(zDEVDfmk, 100 μM) or small interfering RNA (si-cas-3) for 24 hours. **(a)** Cell viability was measured by the CCK-8 assay. **(b)** Gel images of cleaved caspase-8 (cl-cas-8), caspase-3 (cas-3), cleaved caspase-3 (cl-cas-3), γH2AX, full length and N-ternimal of GSDME were obtained by Western blot. (**c, d**) Cell death was analyzed by flow cytometry with annexin V/PI dyes. **(e)** LDH and **(f)** IL-1β levels were measured with culture supernatant. **(g)** Alteration of cell morphology was shown by bright-field microscopy. Experiments were repeated three times independently. Ctrl, control. * , $P < 0.05$.

Fig. 6 Effects of ROS, pJNK and NF-κB on birinapant and lobaplatin-induced pyroptosis in NPC cells.

(a,b) The ROS level and protein expression of p-JNK, JNK, p-IKBα, IKBα, NIK and p100/p52 in CNE-1 and S26 cells treated with 1 μM birinapant (B1) and/or 10 μM lobaplatin (L10), were measured by flow cytometery and Western blot analyses, respectively. **(c-f)** The effects of ROS scavenger (NAC, 5 mM), JNK inhibitor (SP600125, 10 μM) or NF-κB inhibitor (BMS-345541, 1μM) on the cell viability of CNE-1 and S26 cells in the presence of 1 μM birinapant (B1) and/or 10 μM lobaplatin (L10) were assessed via CCK-8 assay. **(g)** CNE-1 and S26 cells were treated with 1 μM birinapant (B1) and 10 μM lobaplatin (L10) in the presence or absence of 500 mM NAC for 24 hours. Then the gel images of total and cleaved caspase-3 (cas-3 and cl-cas-3), full length and N-ternimal of GSDME (GSDME-F and GSDME-N) were obtained by Western blot. **(h)** LDH and **(i)** IL-1β levels were measured with culture supernatant.

Experiments were repeated three times independently. Ctrl, control. * , $P < 0.05$. n.s., not significant.

Fig. 7 Pyroptosis of NPC cells induced by birinapant and lobaplatin depends on Ripoptosome.

CNE-1 and S26 cells were treated with 1 μM birinapant (B1) and 10 μM lobaplatin (L10) in the presence or absence of pan-caspases inhibitor (zVADfmk, 100 μM), ROS scavenger (NAC, 5 mM), small interfering RNA against RIPK1 (siRIPK1) or scramble control (siNC) as indicated for 24 hours. **(a, b)** The formation of Ripoptosome (RIPK1/FADD/caspase-8) was detected by CoIP and Western blot analyses. **(c, d)** Dead ratios of CNE-1 and S26 cells were detected by annexin V/PI cytometry. **(e)** Gel images of RIPK1, total and cleaved caspase-8 (cas-8 and cl-cas-8), total and cleaved caspase-3 (cas-3 and cl-cas-3), full length and N-ternimus of GSDME (GSDME-F and GSDME-N) and γH2AX were detected by Western blot. **(f)** Alteration of cell morphology was shown by bright-field microscopy. **(g)** LDH and **(h)** IL-1β levels were measured with culture supernatant. Ctrl, control. * , $P < 0.05$.

Fig. 8 Birinapant enhances the inhibitory effect of lobaplatin on NPC xenografts.

CNE-1 and S26 xenograft mice were intraperitoneally administered with 10 mg/kg birinapant (B) every 3 days and/or 5 mg/kg lobaplatin (L) every 6 days for 3 weeks. **(a-d)** Tumor volume and body weight were measured every 3 days. **(e-h)** After execution, tumors were pictured and weighted. **(i)** Gel images of cIAP1, cIAP2, XIAP,

549 total and cleaved caspase-3 (cas-3 and cl-cas-3), full length and free N-ternimus of
550 GSDME (GSDME-F and GSDME-N) and γH2AX in tumors were measured by
551 Western blot. **(j)** The H&E staining of liver and kidney paraffin slices. Ctrl, control.
552 * , $P < 0.05$.

553

554 **Graphical abstract**

555 Schematic illustration of the anti-NPC mechanism of lobaplatin in combination with
556 birinapant**.**

557 **Author contributions**
558
559 **Zide Chen**, prepared the materials, performed the experiments and analyzed the data,
560 wrote the original draft
561 **Gang Xu,** prepared the materials, performed the experiments and analyzed the data.
562 **Dong Wu,** prepared the materials, performed the experiments and analyzed the data.
563 **Shihai Wu,** prepared the materials, performed the experiments and analyzed the data.
564 **Long Gong,** prepared the materials, performed the experiments and analyzed the data.
565 **Zihuang Li,** performed the experiments and analyzed the data.
566 **Guanghong Luo,** performed the experiments and analyzed the data.
567 **Jian Hu,** performed the experiments and analyzed the data.
568 **Jian Chen,** performed the experiments and analyzed the data.
569 **Xiaoting Huang,** performed the experiments and analyzed the data.
570 **Chengcong Chen,** performed the experiments and analyzed the data.
571 **Zhenyou Jiang,** conceived and designed the study, writing-reviewing and editing.
572 **Xianming Li,** conceived and designed the study, writing-reviewing and editing.
573
574 All authors have no conflicts of interest to disclose, and have read and approved the
575 final version of the manuscript.
576
577

578

579 **Table 1. IC50 of lobaplatin, cisplatin or birinapant for NPC cell lines**

IC50 (μM, 95% CI)	24 hours	48 hours
Lobaplatin/CNE-1	34.568 [n.s., *]	5.739 [n.s., *]

Lobaplatin/S26	35.108 n.s., *	11.676 n.s., *
Lobaplatin/HONE-1	78.938	14.629
Lobaplatin/SUNE-1	172.322	14.057
Lobaplatin/CNE-2	34.576	8.632
Lobaplatin/HL-7702	205.192	21.758
Cisplatin/CNE-1	30.018	5.708
Cisplatin/S26	48.923	15.248
Birinapant/CNE-1	-	25.556
Birinapant/S26	1.866	0.461
Birinapant/HONE-1	114.573	67.993
Birinapant/SUNE-1	97.169	47.363
Birinapant/CNE-2	49.445	0.402

580 n.s., not statistically significant between lobaplatin and cisplatin treatments; *, statistically significant
581 between CNE-1 (or S26) and HL-7702 cell lines; -, not value.
582
583

Figure 1

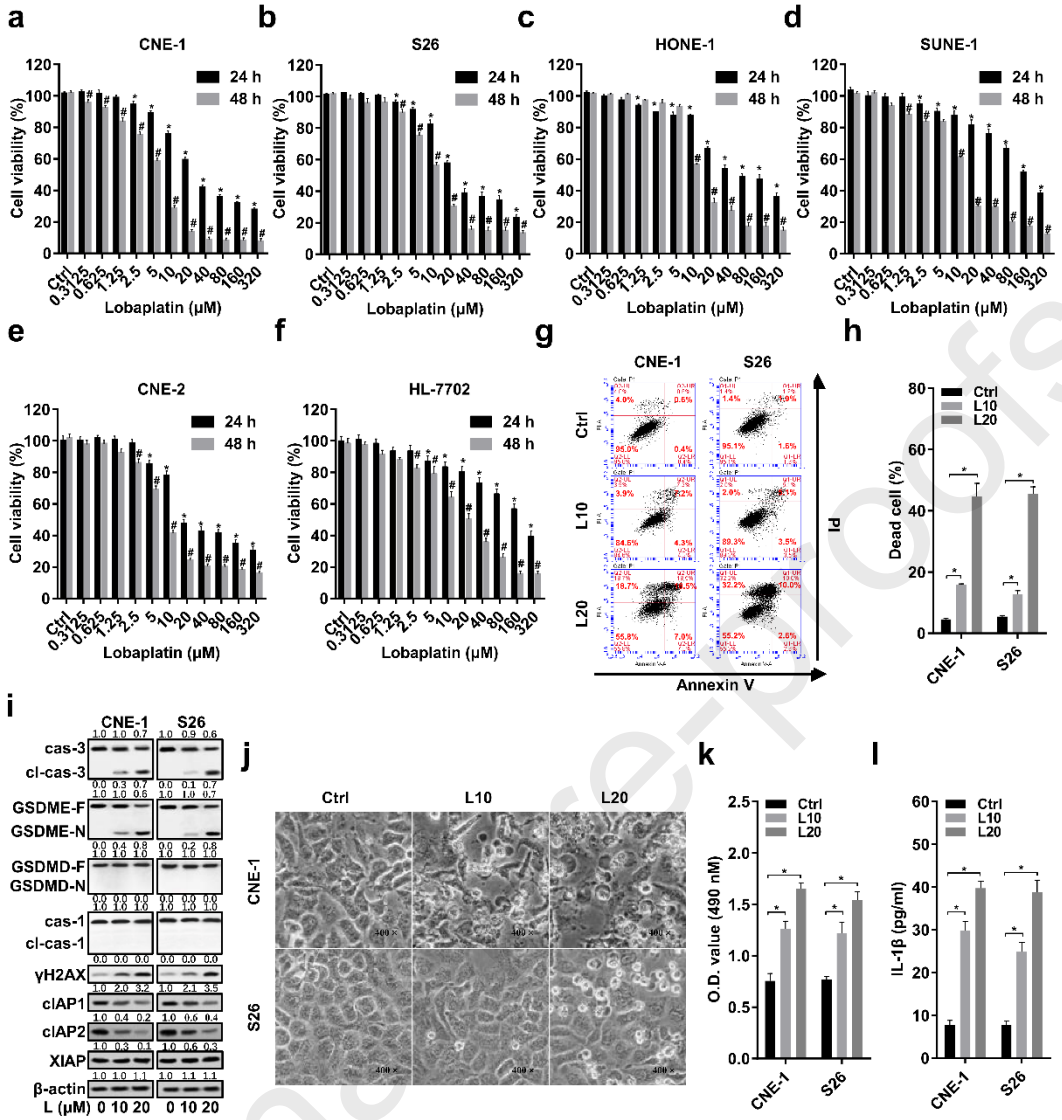

584

Figure 2

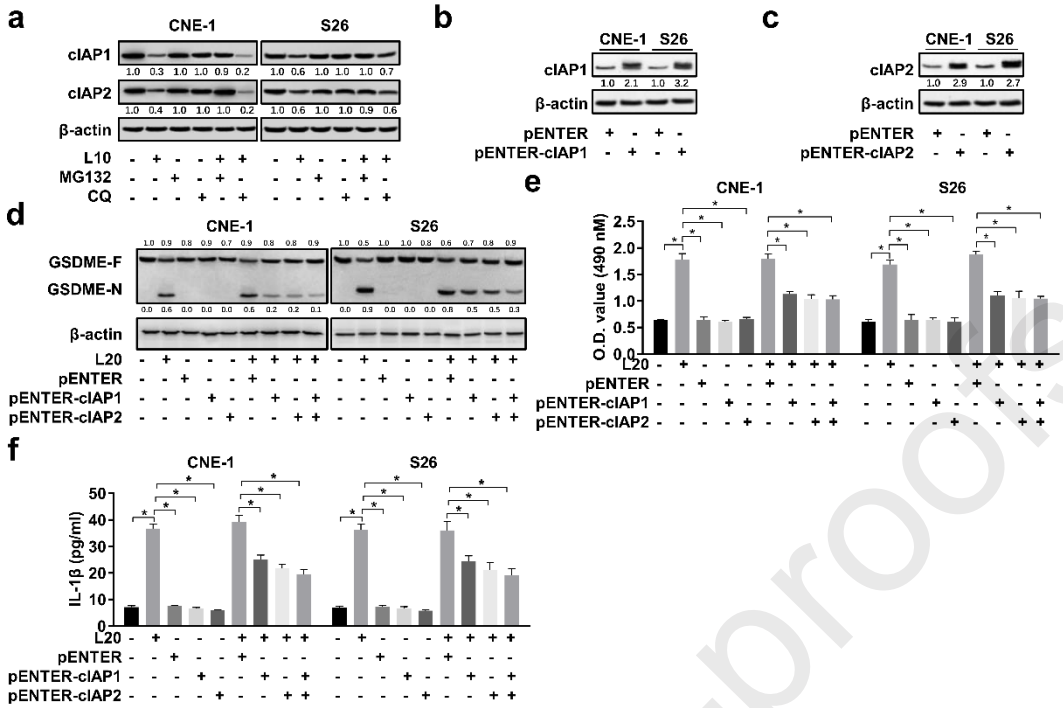

585

Figure 3

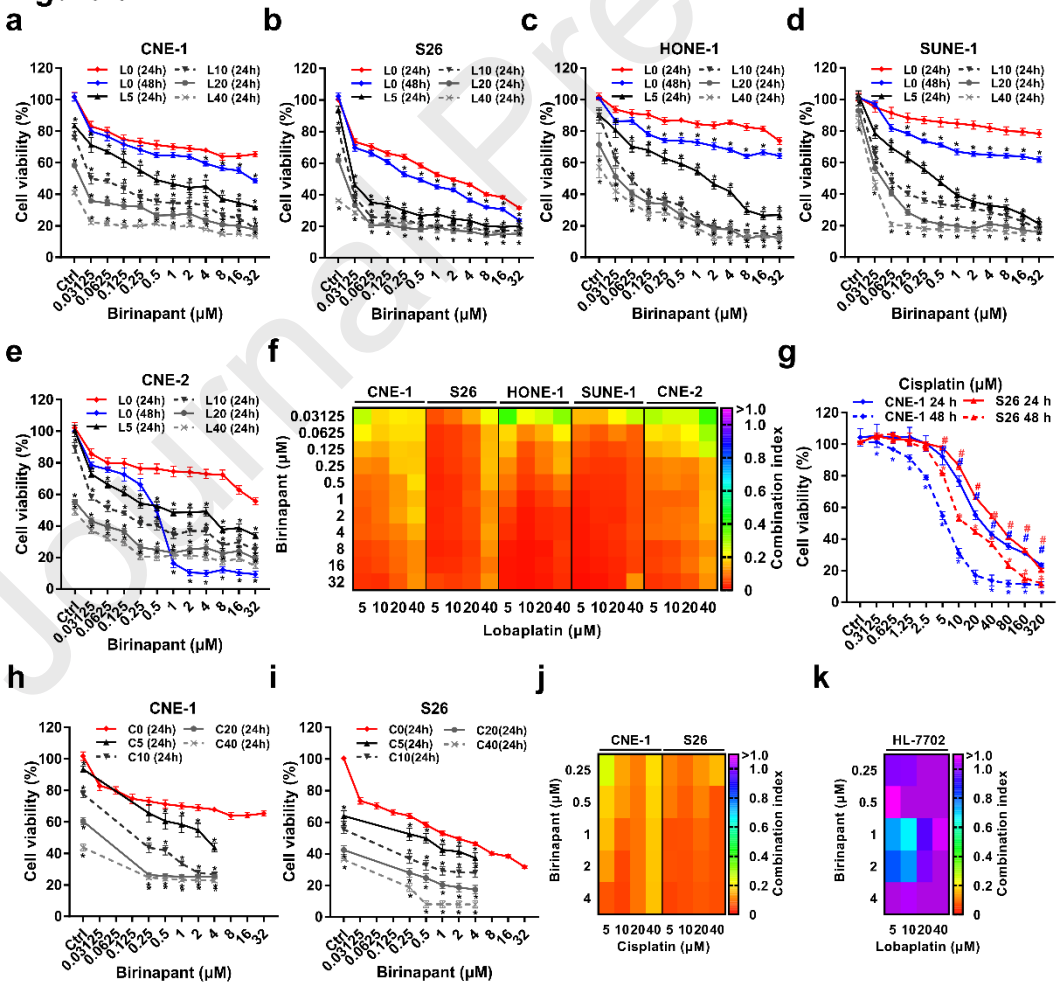

586

Figure 4

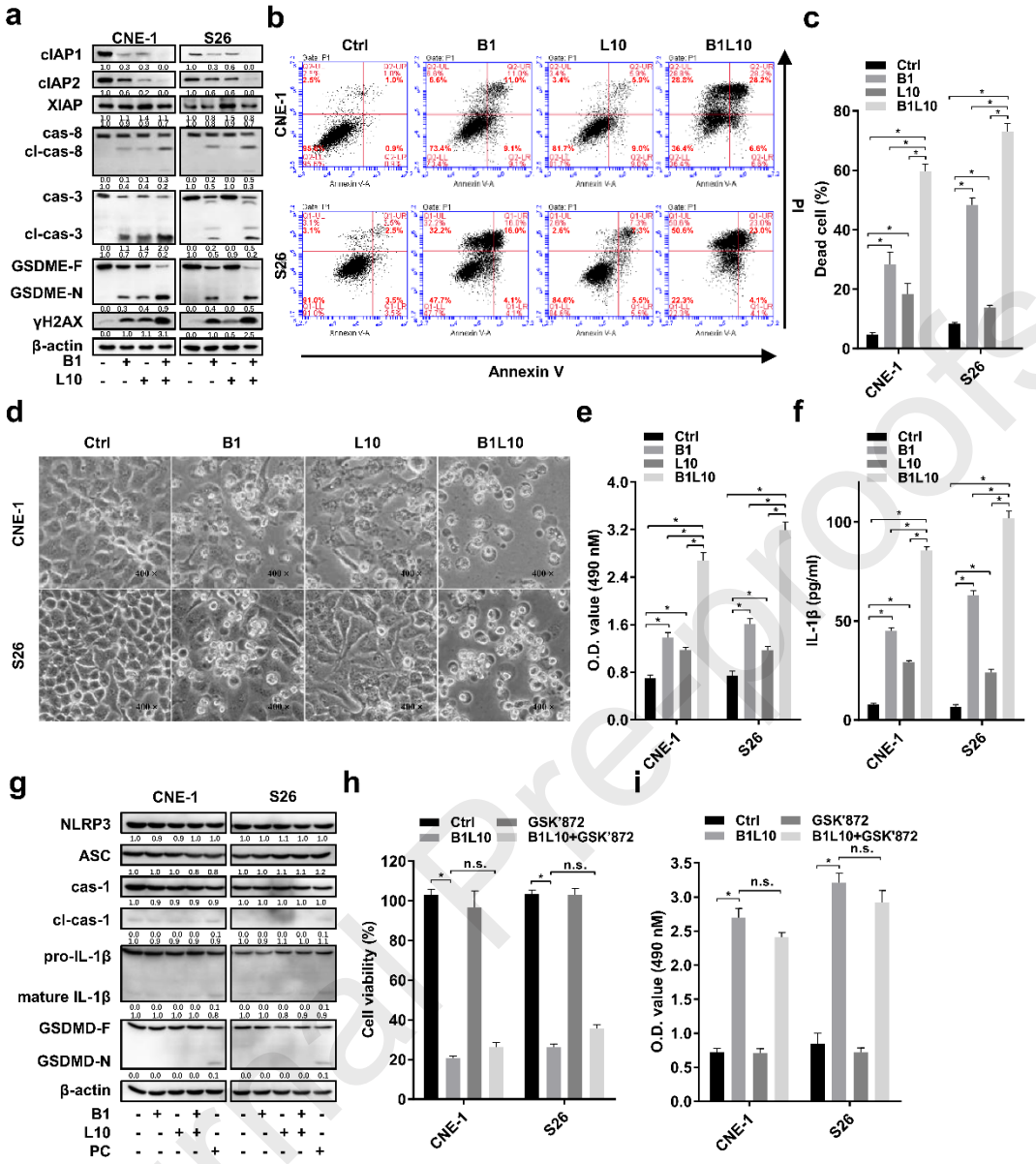

587

Figure 5

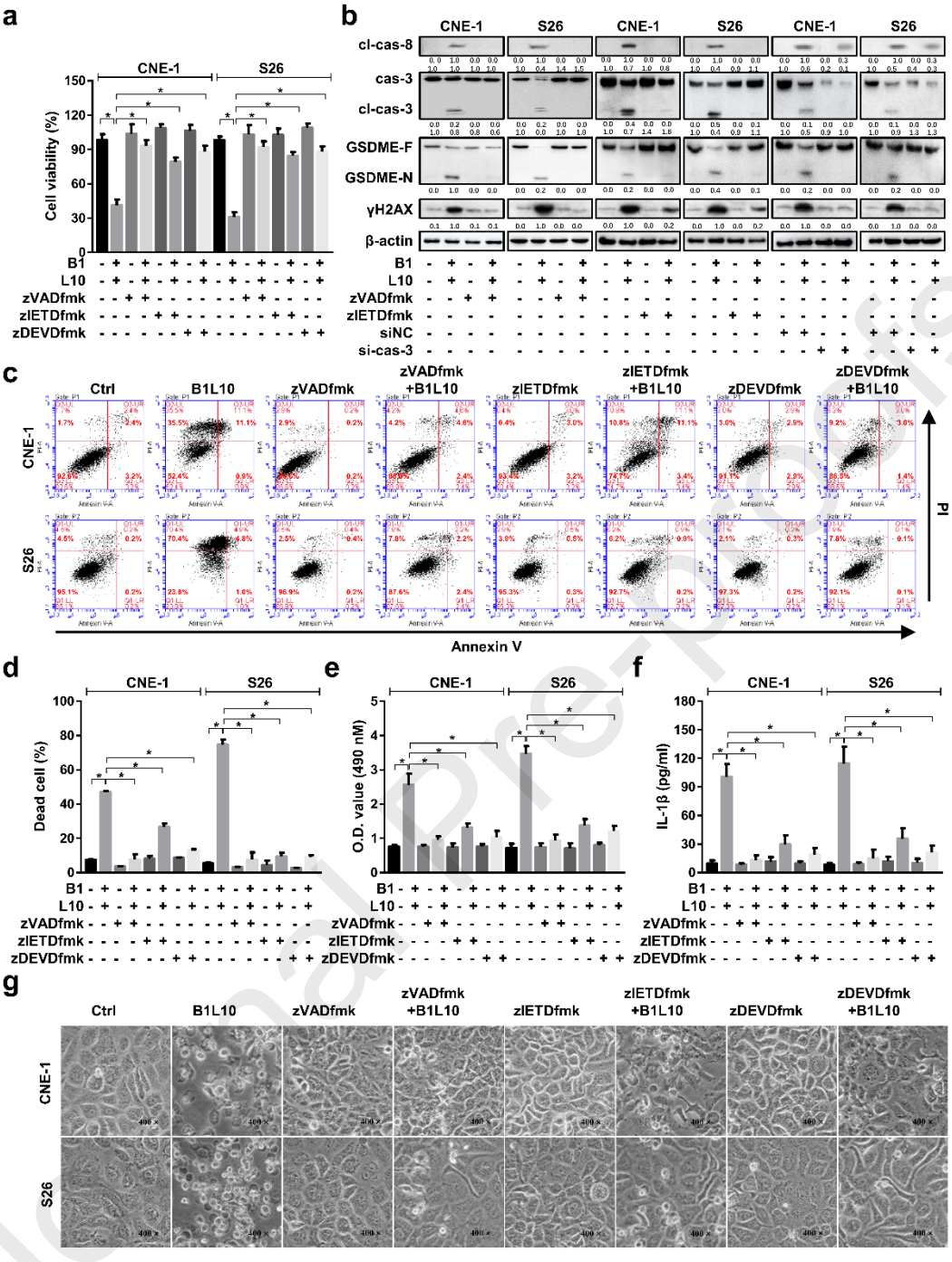
a
CNE-1
S26
Cell viability (%)
B1
L10
zVADfmk
zIETDfmk
zDEVDfmk
b
CNE-1
S26
cl-cas-8
cas-3
cl-cas-3
GSDME-F
GSDME-N
γH2AX
β-actin
B1
L10
zVADfmk
zIETDfmk
siNC
si-cas-3
c
Ctrl
B1L10
zVADfmk
zVADfmk +B1L10
zIETDfmk
zIETDfmk +B1L10
zDEVDfmk
zDEVDfmk +B1L10
CNE-1
S26
PI
Annexin V
d
Dead cell (%)
e
O.D. value (490 nM)
f
IL-1β (pg/ml)
g
Ctrl
B1L10
zVADfmk
zVADfmk +B1L10
zIETDfmk
zIETDfmk +B1L10
zDEVDfmk
zDEVDfmk +B1L10
CNE-1
S26

588

Figure 6

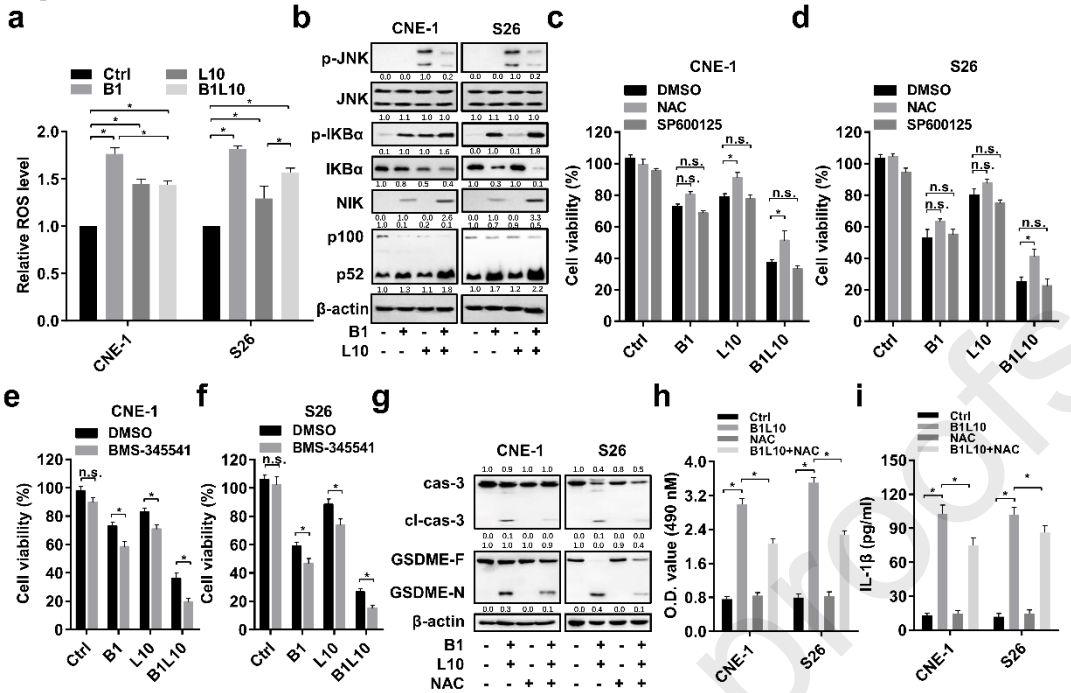

589

Figure 7

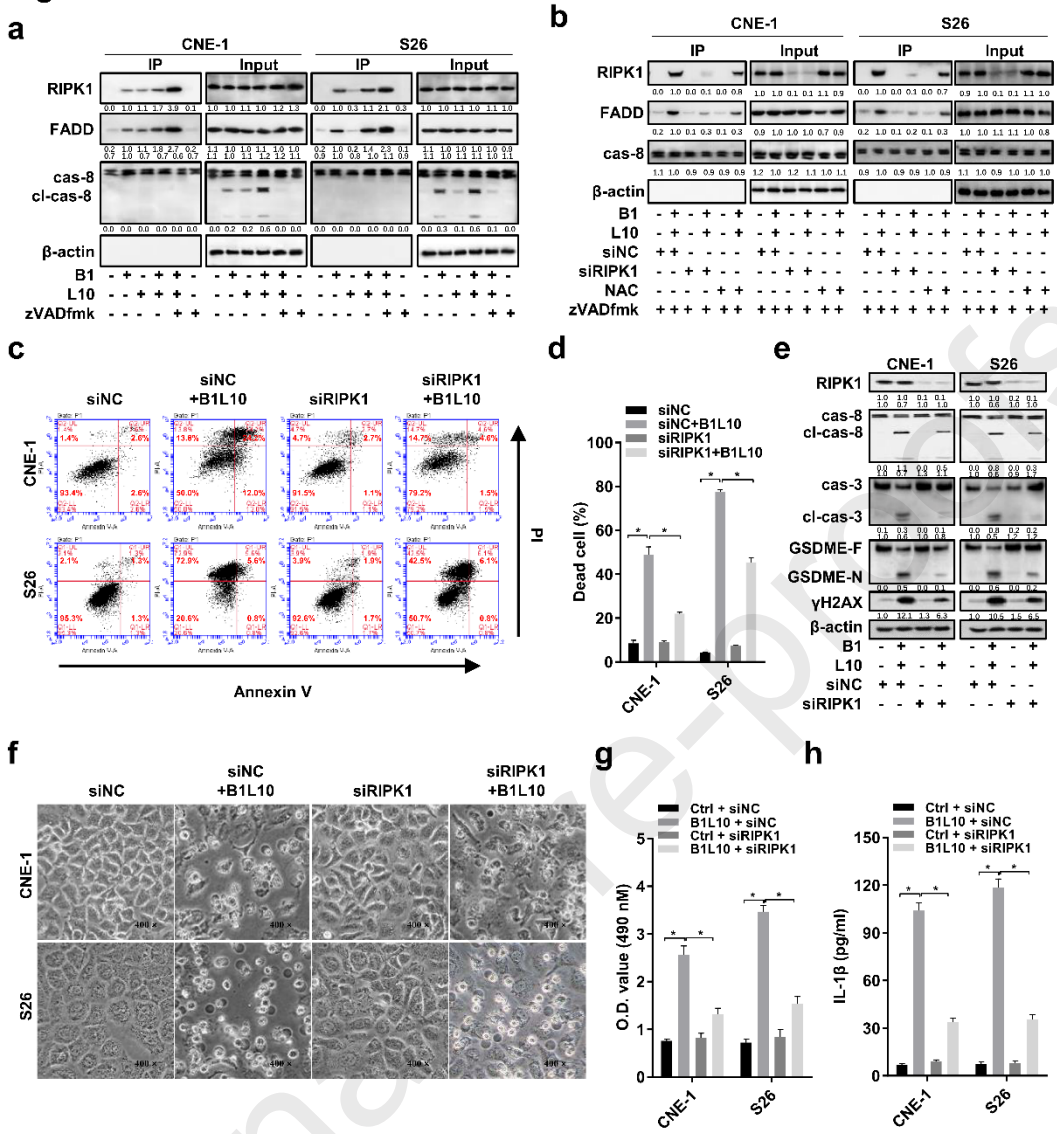

590

Figure 8

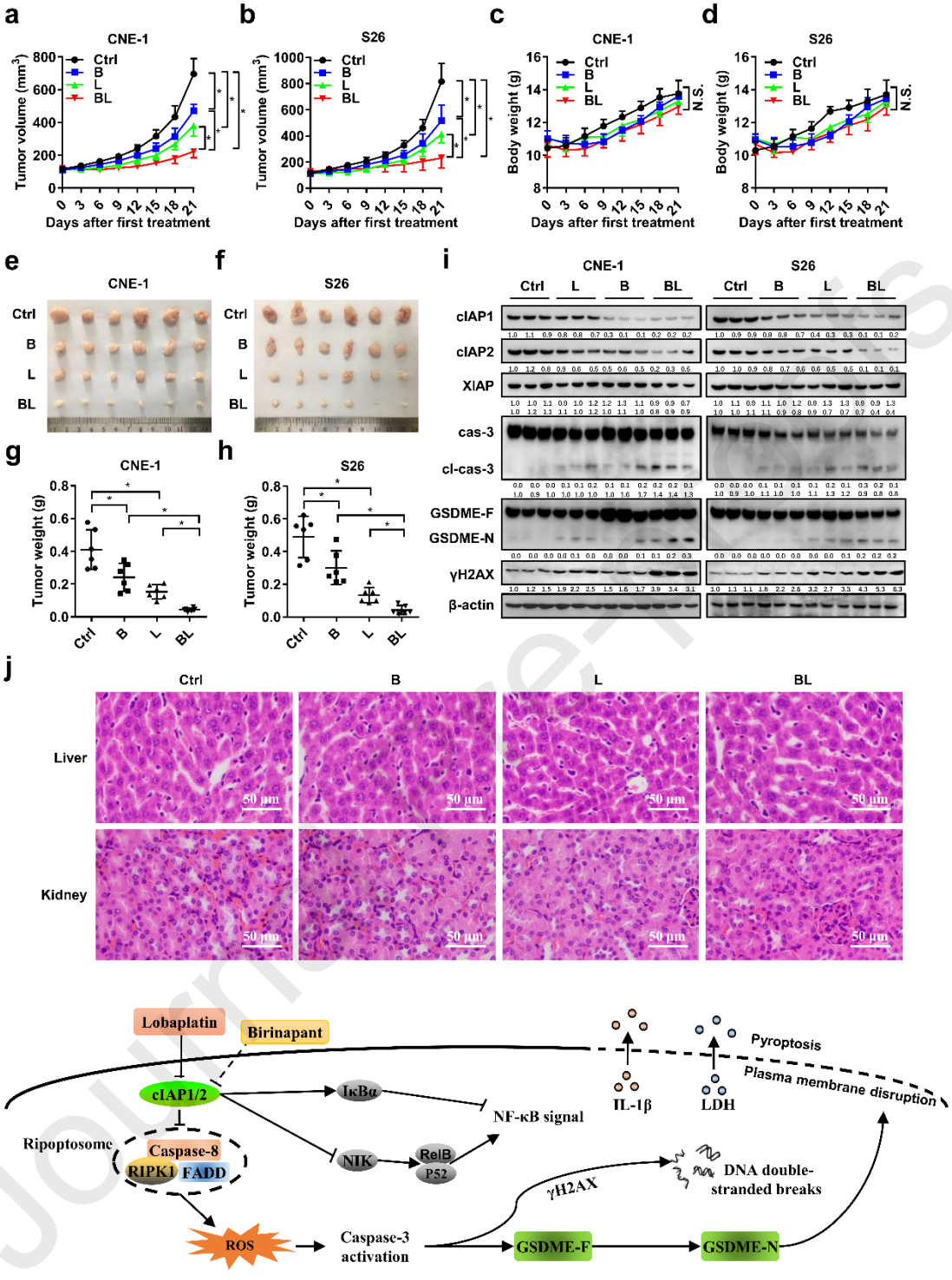
a
CNE-1
Tumor volume (mm3)
Days after first treatment
Ctrl
B
L
BL
b
S26
c
CNE-1
Body weight (g)
N.S.
d
S26
e
CNE-1
f
S26
g
CNE-1
Tumor weight (g)
h
S26
i
CNE-1
S26
cIAP1
cIAP2
XIAP
cas-3
cl-cas-3
GSDME-F
GSDME-N
γH2AX
β-actin
j
Liver
Kidney
50 μm
Lobaplatin
Birinapant
cIAP1/2
IκBα
NF-κB signal
Ripoptosome
Caspase-8
RIPK1
FADD
NIK
RelB
P52
ROS
Caspase-3 activation
γH2AX
DNA double-stranded breaks
GSDME-F
GSDME-N
IL-1β
LDH
Pyroptosis
Plasma membrane disruption